Stable Immobilization of Enzyme on Pendant Glycidyl Group-Modified Mesoporous Carbon by Graft Polymerization of Poly(glycidyl methacrylate)

Isao Shitanda,[*1,2,#] **Takanao Kato,**[1,#] **Ryo Suzuki,**[1] **Tatsuo Aikawa,**[1] **Yoshinao Hoshi,**[1] **Masayuki Itagaki,**[1,2] **and Seiya Tsujimura**[2,3,#]

[1]Department of Pure and Applied Chemistry, Faculty of Science and Technology, Tokyo University of Science, 2641 Yamazaki, Noda, Chiba 278-8510, Japan

[2]Research Institute for Science and Technology, Tokyo University of Science, 2641 Yamazaki, Noda, Chiba 278-8510, Japan

[3]Division of Material Science, Faculty of Pure and Applied Science, University of Tsukuba, 1-1-1 Tennodai, Tsukuba, Ibaraki 305-5358, Japan

E-mail: shitanda@rs.noda.tus.ac.jp

Isao Shitanda
Isao Shitanda received his PhD (Engineering) from The University of Tokyo in 2006. He is currently a junior Associate Professor in the Department of Pure and Applied Chemistry, Faculty of Science and Technology, Tokyo University of Science (TUS), Japan. His research interests include electrochemical sensors, actuators, biosensors, and biofuel cells.

Abstract

Poly(glycidyl methacrylate) (poly(GMA)) bearing pendant glycidyl groups, grafted on the surface of MgO-templated carbon (MgOC), is useful for forming strong multipoint covalent bonds with amino functional groups on the surface of flavin adenine dinucleotide-dependent glucose dehydrogenase (FAD-GDH) molecules. The immobilized FAD-GDH can generate glucose-oxidation catalytic current using 1,2-naphthoquinone (12NQ) as the redox mediator, which is also captured on the electrode surface. The catalytic current is more stable than that obtained using the FAD-GDH-MgOC electrode without poly(GMA) because the leaching of FAD-GDH and 12NQ is suppressed by the enzyme capping effect.

Keywords: Biofuel cell | Graft polymerization | Immobilization of enzyme

1. Introduction

Enzymatic biofuel cells (EBFCs) are a type of fuel cell employing enzymes, instead of conventional noble metal catalysts.[1,2] The working principle is the same as that in conventional polymer electrolyte membrane fuel cells, i.e., the fuel is oxidized at the anode, and the released electrons migrate to the cathode, where they combine with oxygen to form water.

EBFCs are promising for sustainable green energy applications; however, they are currently at an early stage of their development, with many yet-to-be-resolved fundamental scientific and engineering problems. Two such critical problems are their short lifetime and poor power density.

The electroenzymatic reaction can be categorized into two types. One is the direct electron transfer (DET) reaction, in which the electron is transferred directly between the electrode and the active site of the enzyme adsorbed on the electrode surface with suitable orientation. The other type is the mediated electron transfer (MET) reaction, in which, contrary to DET reactions, the electron is shuttled by redox molecules (called redox mediators) between the electrode surface and the redox active site buried in the protein shell. The co-immobilization of the mediator and the enzyme on the electrode surface is technically more difficult in the MET reaction than in the DET reaction for device applications. Briefly, the mediator should be immobilized in the enzyme layer without losing its electrochemical activity and electron mobility between the enzyme active site and the electrode surface.

These are in turn related to factors determining the stability of the enzyme on the electrode surface, including the structural stability of the enzyme, desorption of enzyme from the electrode surface, and decrease in the amount and activity of the

redox mediator, which shuttles electrons between the enzyme and the electrode surface.

Solving the above-mentioned problems using porous carbon materials is a promising approach.[3–18] To date, various carbon materials, including carbon nanotubes, carbon black, and porous carbon, have been developed for use in EBFCs. Using these kind of carbon materials can improve the effective electrode surface area, leading to increased current density and output density. Supporting enzymes on these types of porous materials is expected to lead to increased output density.

Willner et al. reported that the long-term stability is significantly improved by preventing mediator leaching from the electrode by capping mesopores with glucose oxidase (GOx) after supporting the mediator in the mesoporous carbon material.[12] Fujita also developed a hierarchical-structured porous carbon material containing both small and large pores, which adsorb the mediator and the enzyme, respectively, preventing mediator leakage.[19] We developed carbon materials with controlled pore sizes, carbon aerogels, and MgO-templated carbon, and electrodes designed from such pore-size-controlled carbon materials showed higher performance than nano-structured carbon electrodes (e.g. carbon black).[4,5,9,11,20,21]

The enzymes physically adsorbed inside the porous carbon gradually leach from the carbon surface after long-term operation or during the replacement of the fuel solution. Therefore, cross-linkers such as glutaraldehyde[12] and redox polymer hydrogel such as Os polymer hydrogel[22] were used to prevent the enzymes from leaching from the carbon surface. Besides, they are also effective in covalently linking the enzyme on the carbon surface.[19,23] For example, N-hydroxysuccinimide-activated pyrene was sometimes modified on the carbon surface to provide long-term stability. As mentioned above, developing strategies for the stable immobilization of enzyme on the carbon surface still remains a major challenge.

In this study, to prevent enzyme leakage, the enzyme was immobilized on the carbon material via multipoint covalent bonding; the grafting of polymers bearing pendant glycidyl groups was achieved by the polymerization of glycidyl methacrylate (GMA), initiated by electron beam irradiation on the carbon surface. Graft polymerization initiated by electron beam irradiation was previously conducted on plastic surfaces, such as polyethylene[24,25] and polypropylene;[26,27] however, there are no reports on its application to porous carbon modification. The advantage of this technique is that the carbon material surface of as well as the inner surface of the pores can be activated. Poly(GMA) grafted onto the porous carbon surface can react with the amino functional groups on the enzyme surface. Thus, an enzyme is expected to be immobilized on the carbon surface easily and stably by merely dropping an enzyme solution on the carbon surface.

In this study, poly(GMA) was first grafted on the MgOC surface, following which the mediator (1,2-naphthoquinone; 12NQ) was introduced in the MgOC. Finally, FAD-GDH was immobilized by linking with epoxy groups on the GMA graft chain (Figure 1), which suppresses mediator leaching from the MgOC pores by the capping effect of the enzyme. This technique dramatically improved the stabilities of the FAD-GDH-modified MgOC electrode for long-term storage and continuous operation.
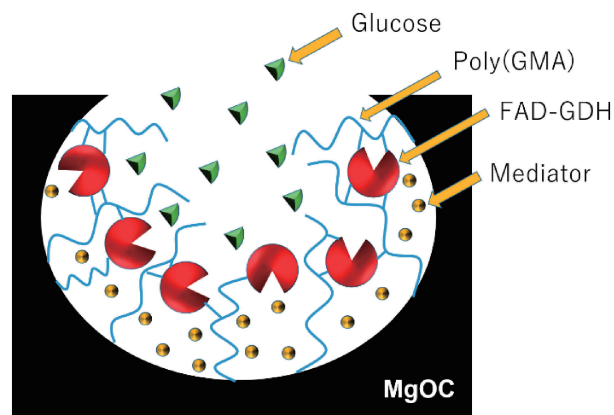

Figure 1. Schematic of FAD-GDH-capped poly(GMA)-modified MgOC (FAD-GDH-immobilized GMgOC). The mediator (1,2-naphthoquinone; 12NQ) was introduced in the MgOC pore. FAD-GDH was immobilized on the MgOC surface via multipoint covalent bonding, along with grafting of polymers bearing pendant glycidyl groups.
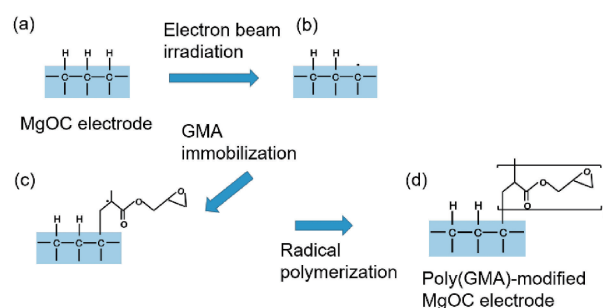

Figure 2. Schematic of graft polymerization of poly(GMA) on MgOC surface.

2. Experimental

2.1 Reagents and Equipment. FAD-GDH (205 U/mg) was purchased from Amano Enzyme (Japan). 12NQ was purchased from Kanto Chemical (Japan). GMA, dimethylsulfoxide (DMSO), acetonitrile, 1-methyl-2-pyrrolidone (NMP), disodium hydrogen phosphate, sodium dihydrogen phosphate, and D(+)-glucose were purchased from Wako Pure Chemical Industries (Japan). Triton X-100 was purchased from Alfa Aesar. Kureha KF Polymer #9305 (PVdF) was purchased from Kureha (Japan). MgOC (average pore diameter = 100 nm, CNovel® MJ(3)-100-00) was purchased from Toyo Carbon (Japan).

2.2 GMA Polymerization Initiated by Electron Beam Irradiation on MgOC. This polymerization is schematically shown in Figure 2. Poly(GMA) was modified on the MgOC surface by graft polymerization. MgOC (1.5 g) and an oxygen scavenger were placed in an airtight bag filled with Ar gas. Electron beam irradiation was performed at 100 kGy by Japan Irradiation Service (Japan) to generate radicals on the MgOC surface. The electron-beam-irradiated MgOC was mixed with a solution containing 20 wt.% GMA and 80 wt.% DMSO. The mixed solution was stirred for 24 h at 80 °C. The product, poly(GMA)-modified MgOC (GMgOC) was washed with DMSO, dried at 100 °C (48 h), and analyzed by Fourier-transform infrared (FT-IR) spectroscopy (FT/IR-6100, JASCO)

over the range 4000–500 cm^{-1} at a resolution of 4.0 cm^{-1}.

2.3 Preparation of the GMgOC Electrode and Immobilization of FAD-GDH. GMgOC (40 mg), PVdF (100 μL), and NMP (70 μL) were mixed in a sample tube fitted with a vortex mixer. The carbon ink was then coated on a glassy carbon electrode (diameter = 3 mm, ALS, Japan) and dried at 40 °C for 24 h. As a control, MgOC without poly(GMA) was also modified on a glassy carbon electrode.

An acetonitrile solution of 12NQ (5 μL, 10 mM) was dropped on the electrode surface and dried at room temperature for 1 h. Then, 5 μL of 10 mM phosphate buffer solution (pH 7.0), containing 20 units FAD-GDH and 0.015% Triton X-100, was cast on the GMgOC or MgOC-modified electrode surface and dried at room temperature for 1 h.

2.4 Electrochemical Evaluation of FAD-GDH-Immobilized Electrodes. Cyclic voltammetry (CV) and chronoamperometry (CA) were performed by the three-electrode method using a potentiostat (ALS/DY 2325) in a 1 M phosphate buffer solution (pH 7.0) containing 100 mM glucose at 25 °C. A Pt wire and a commercially available saturated KCl|Ag|AgCl electrode were used as the counter and reference electrodes, respectively. CV was performed over a potential range from −0.4 V to +0.4 V at 10 mV s^{-1}. The potential for CA was set at +0.3 V. The long-term storage stabilities of the prepared electrodes were evaluated daily in a 1 M phosphate buffer solution (pH 7.0) containing 100 mM glucose by CV. The prepared electrodes were stored in a 10 mM phosphate buffer solution (pH 7.0) at 4 °C.

3. Results and Discussion

3.1 Graft Polymerization of GMA on the MgOC Surface. The grafted poly(GMA), bearing pendant glycidyl groups, is useful for forming strong multipoint covalent attachment with different nucleophiles (e.g. amino, thiol, hydroxyl groups) on the surface of enzyme molecules.[28,29] The formation of poly-(GMA) was confirmed from the FT-IR spectrum of GMgOC (Figure 3), which shows peaks due to C=O stretching vibration derived from the carbonyl group near 1735 cm^{-1}, and C-O-C symmetric stretching vibration derived from the epoxy group near 1150 cm^{-1}, both attributed to poly(GMA). Thermogravimetric analysis revealed that the grafting rate was 10.0% (data not shown).

3.2 Electrochemical Evaluation of the FAD-GDH-Immobilized GMgOC Electrode. Figure 4 shows the cyclic voltammograms (25 cycles) of the FAD-GDH-immobilized GMgOC electrode in quiescent 1 M phosphate buffer solution in the presence of 100 mM glucose (pH 7.0, 25 °C) (solid curves) and in the absence of glucose (dashed curve). The catalytic wave was not observed in the absence of glucose. Oxidation and reduction peaks ascribed to the redox reaction of 12NQ were observed at −0.07 V. The shape of the cyclic voltammogram of the MgOC electrode indicates that 12NQ was stably immobilized on the MgOC surface via π-π interactions. The peak current of 12NQ was not drastically changed over 25 cycles (Figure S1). On the other hand, the corresponding peak currents of 12NQ on the GMgOC electrode decreased to 70% of the initial value after 10 cycles; however, no further change in peak current was observed, even after 2 weeks of storage in buffer solution. These results suggest that 12NQ was
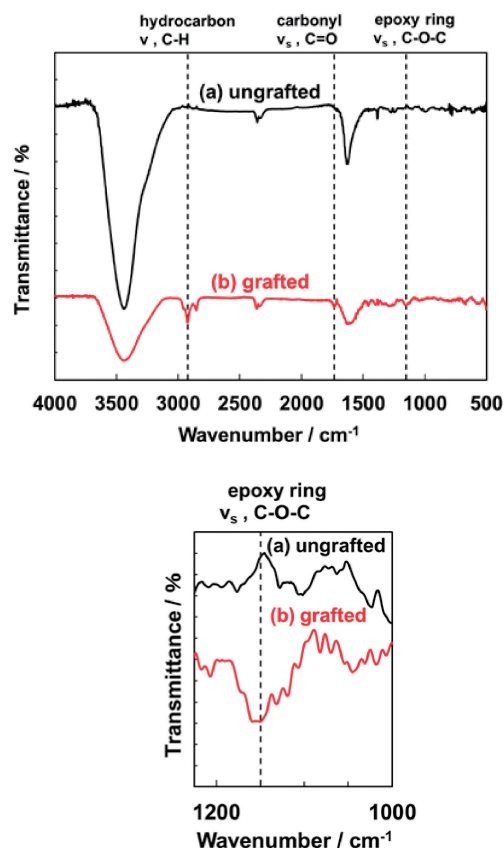

Figure 3. FT-IR spectra of (a) MgOC (ungrafted), (b) GMgOC (10.0% grafted). The lower figure is an enlarged view.
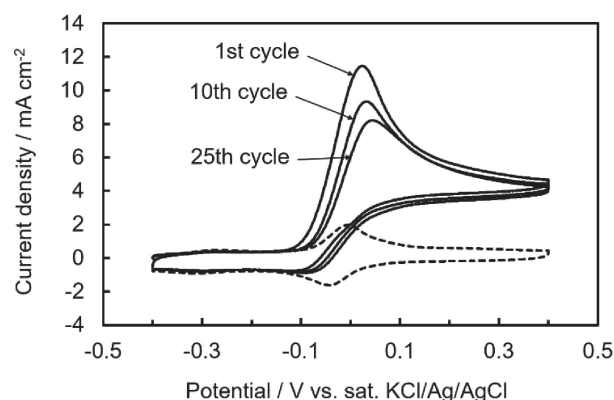

Figure 4. Cyclic voltammograms (25 cycles) of FAD-GDH-immobilized GMgOC electrode in quiescent 1 M phosphate buffer solution in the presence of 100 mM glucose (pH 7.0, 25 °C) (solid curves) and in the absence of glucose (dashed curve). No catalytic wave was observed in the absence of glucose.

not directly adsorbed on the MgOC surface, because poly-(GMA) was grafted on the surface; therefore, some part of 12NQ leached to the solution, while the rest remained stably in the carbon, specifically in the poly(GMA) layer due to enzyme capping effect (Figure 1).

In the presence of glucose, glucose-oxidation catalytic currents were observed for both electrodes. This result indicates
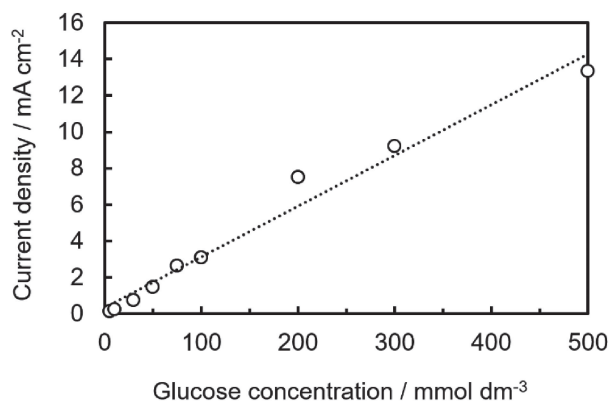
Figure 5. Relationship between glucose concentration and current density of the FAD-GDH-immobilized GMgOC electrode.

Figure 6. Changes in normalized current density of the FAD-GDH-immobilized GMgOC electrode ($\square$) and FAD-GDH-immobilized MgOC electrode ($\bigcirc$), as estimated from the cyclic voltammograms (25 cycles) obtained in 1 M phosphate buffer solution containing 100 mM glucose at +0.3 V (as shown in Figure 4).

Figure 7. Time-current curves of the FAD-GDH-immobilized GMgOC electrode (solid curve) and FAD-GDH-immobilized MgOC electrode (dashed curve) obtained in 1 M phosphate buffer solution containing 100 mM glucose at 0.3 V for 12 h.

that the catalytic activity of FAD-GDH was not lost during its immobilization on the GMgOC surface and mass transfer of glucose from the bulk solution to the active site of FAD-GDH was also not inhibited. The maximum catalytic currents for FAD-GDH-immobilized MgOC and GMgOC electrodes after the first cycle were 7.8 mA cm^{-2} and 11.4 mA cm^{-2}, respectively, but the diffusion-tailed current at 0.4 V was almost the same (4 mA cm^{-2}). The diffusion-limited current density depended on the glucose diffusion rate in the MgOC mesopore, indicating that sufficient FAD-GDH was immobilized inside the pores of MgOC and that the glucose consumption rate at the electrode surface is much higher than the flux of glucose.

The relationship between the glucose concentration and current density of the FAD-GDH-immobilized GMgOC electrode was studied in detail by CA at 0.3 V using 1 M phosphate buffer containing 10–500 mM glucose (Figure 5).

A linear relationship between the glucose concentration and current density was obtained even using 500 mM glucose solution, indicating that the amounts of immobilized FAD-GDH and 12NQ in the GMgOC were sufficient to show enough catalytic activity for observing glucose-diffusion limited current even at high glucose concentrations.

Interestingly, we can see a clear difference in the short-term stabilities of the electrodes evaluated by 25 cycles of CV. The changes in the current density of the prepared electrodes at +0.3 V (Figure 4) were plotted for each cycle (Figure 6).

The normalized current density was maintained at 95% even after 25 cycles for the FAD-GDH-immobilized GMgOC electrode. On the other hand, only 51% of the current density was retained when the FAD-GDH-immobilized MgOC electrode was used. Considering the change in the redox peak of 12NQ in the absence of glucose, the decrease in the catalytic current on the MgOC electrode was ascribed to enzyme leaching, which was suppressed using the GMgOC electrode.

3.3 Evaluation of Long-Term Stability of the FAD-GDH-Immobilized GMgOC Electrode. Figure 7 shows the time-current curves of the prepared electrodes obtained in 1 M phosphate buffer solution containing 100 mM glucose at 0.3 V for 12 h. In the absence of poly(GMA), the current decreased quickly (dashed curve). The current density obtained using the FAD-GDH-immobilized GMgOC electrode was 0.8 mA cm^{-2}, 3.5 times higher than that obtained using FAD-
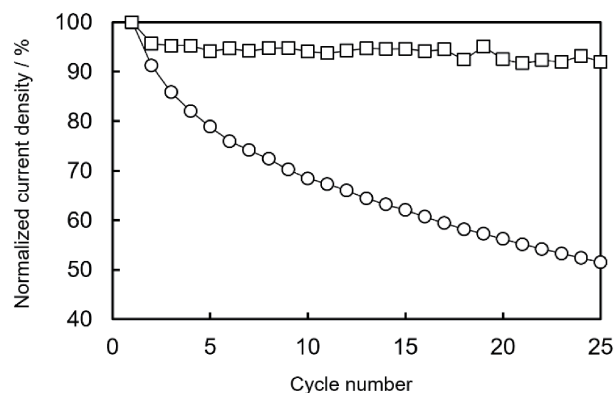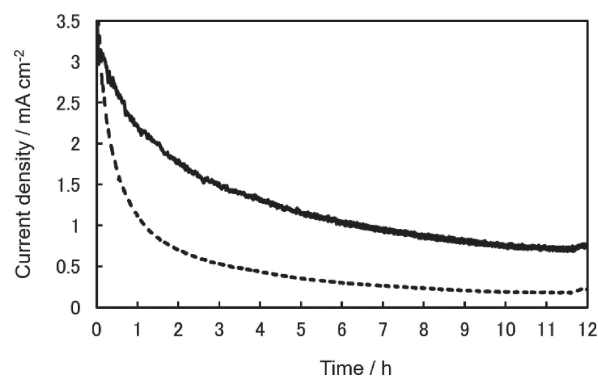
GDH-immobilized MgOC electrode after 12 h (solid curve). Half-life times of the MgOC and GMgOC electrodes were 0.5 and 3 h, respectively.

The long-term storage stabilities of the prepared electrodes were evaluated by daily CV measurements. A plot of the 0.3 V current value in each cyclic voltammogram is shown in Figure 8.

The FAD-GDH-immobilized GMgOC electrode retained 100% stability over 1 week. On the contrary, the stability of the FAD-GDH-immobilized MgOC electrode decreased drastically, and less than 10% of the initial electrochemical activity was retained after 1 week because the pore size of the MgOC used herein (~100 nm) was much larger than that in FAD-GDH. Thus, the enzyme was gradually leached to the bulk solution with time for the MgOC electrode. The stability of the FAD-GDH-immobilized MgOC electrode gradually decreased with time and became ~60% after storage for 2 weeks, probably due to the deactivation of FAD-GDH or mediator leaching. However, we observed that the peak current of 12NQ in the absence of glucose decreased to ~10% of the initial value after storage for 15 days.
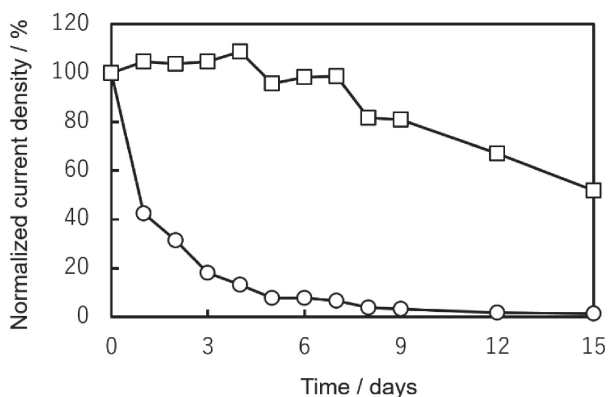
Figure 8. Long-term storage stabilities of the FAD-GDH-immobilized GMgOC electrode (□) and FAD-GDH-immobilized MgOC electrode (○), as evaluated by daily CV measurements in 1 M phosphate buffer solution containing 100 mM glucose at 0.3 V.

4. Conclusions

In conclusion, the long-term stability of a bioanode was improved drastically using GMgOC with a simple immobilization scheme. The present method is based on the enzyme immobilization on a mesoporous carbon material via multi-point covalent bonding to prevent enzyme leakage. FAD-GDH was successfully immobilized on the GMA graft chain. The FAD-GDH-immobilized MgOC suppressed leaching of 12NQ from the MgOC pores by the capping effect of the FAD-GDH enzyme. The storage stability of the FAD-GDH-immobilized GMgOC electrode was 100% over 1 week. The technique described herein is promising for the stability enhancement of bioelectrodes, particularly because the commercialization of biofuel cells is inevitable in the near future.

Supporting Information

Electrochemical evaluation of the FAD-GDH-immobilized MgOC electrode in quiescent 1 M phosphate buffer solution in the absence of glucose. This material is available on https://doi.org/10.1246/bcsj.20190212.

References

  # These authors contributed equally.

1 S. C. Barton, J. Gallaway, P. Atanassov, *Chem. Rev.* **2004**, *104*, 4867.

2 R. A. Bullen, T. C. Arnot, J. B. Lakeman, F. C. Walsh, *Biosens. Bioelectron.* **2006**, *21*, 2015.

3 K. L. Jiao, Z. P. Kang, B. Wang, S. Q. Jiao, Y. Jiang, Z. Q. Hu, *Electroanalysis* **2018**, *30*, 525.

4 A. Suzuki, N. Mano, S. Tsujimura, *Electrochim. Acta* **2017**, *232*, 581.

5 H. Funabashi, S. Takeuchi, S. Tsujimura, *Sci. Rep.* **2017**, *7*, Article number: 45147.

6 K. Sakai, Y. Kitazumi, O. Shirai, K. Kano, *Electrochem. Commun.* **2016**, *65*, 31.

7 M. Inagaki, M. Toyoda, Y. Soneda, S. Tsujimura, T. Morishita, *Carbon* **2016**, *107*, 448.

8 I. Shitanda, S. Tsujimura, H. Yanai, Y. Hoshi, M. Itagaki, *Electrochemistry* **2015**, *83*, 335.

9 I. Shitanda, H. Nakafuji, S. Tsujimura, Y. Hoshi, M. Itagaki, *Electrochemistry* **2015**, *83*, 329.

10 S. Tsujimura, K. Murata, W. Akatsuka, *J. Am. Chem. Soc.* **2014**, *136*, 14432.

11 K. Murata, W. Akatsuka, S. Tsujimura, *Chem. Lett.* **2014**, *43*, 928.

12 A. Trifonov, K. Herkendell, R. Tel-Vered, O. Yehezkeli, M. Woerner, I. Willner, *ACS Nano* **2013**, *7*, 11358.

13 A. Niiyama, K. Murata, Y. Shigemori, A. Zebda, S. Tsujimura, *J. Power Sources* **2019**, *427*, 49.

14 C. X. Guo, F. P. Hu, X. W. Lou, C. M. Li, *J. Power Sources* **2010**, *195*, 4090.

15 L. Hussein, S. Rubenwolf, F. von Stetten, G. Urban, R. Zengerle, M. Krueger, S. Kerzenmacher, *Biosens. Bioelectron.* **2011**, *26*, 4133.

16 T. G. Perez, S.-G. Hong, J. Kim, S. Ha, *Enzyme Microb. Technol.* **2016**, *90*, 26.

17 B. Reuillard, A. Le Goff, C. Agnes, M. Holzinger, A. Zebda, C. Gondran, K. Elouarzaki, S. Cosnier, *Phys. Chem. Chem. Phys.* **2013**, *15*, 4892.

18 A. J. Gross, M. Holzinger, S. Cosnier, *Energy Environ. Sci.* **2018**, *11*, 1670.

19 S. Fujita, S. Yamanoi, K. Murata, H. Mita, T. Samukawa, T. Nakagawa, H. Sakai, Y. Tokita, *Sci. Rep.* **2014**, *4*, 4937.

20 A. Suzuki, K. Murata, N. Mano, S. Tsujimura, *Bull. Chem. Soc. Jpn.* **2016**, *89*, 24.

21 S. Tsujimura, K. Murata, *Electrochim. Acta* **2015**, *180*, 555.

22 A. Heller, *Acc. Chem. Res.* **1990**, *23*, 128.

23 X. Wang, S. S. Kim, D. Khang, H. H. Kim, C. J. Kim, *Biochem. Eng. J.* **2016**, *112*, 20.

24 S. Machi, I. Kamel, J. Silverman, *J. Polym. Sci., Part A-1: Polym. Chem.* **1970**, *8*, 3329.

25 H. Oraby, M. M. Senna, M. Elsayed, M. Gobara, *J. Appl. Polym. Sci.* **2017**, *134*, 45410.

26 S. Rattan, T. Sehgal, *J. Radioanal. Nucl. Chem.* **2012**, *293*, 107.

27 F. López-Saucedo, G. G. Flores-Rojas, E. Bucio, C. Alvarez-Lorenzo, A. Concheiro, O. González-Antonio, *MRS Commun.* **2017**, *7*, 938.

28 S.-H. Choi, Y. C. Nho, *J. Appl. Polym. Sci.* **1999**, *71*, 999.

29 S.-H. Choi, K.-P. Lee, J.-G. Lee, *Microchem. J.* **2001**, *68*, 205.